

Redox Capacitive Detection of CRP at a Peptide Supported Aptamer Interface

Julia Piccoli ^a, Robert Hein ^b, Afaf H. El-Sagheer^b, Tom Brown^b, Eduardo M. Cilli ^a, Paulo R. Bueno ^{a, #} and Jason J. Davis ^{b,*}

^aInstitute of Chemistry, São Paulo State University (UNESP), Araraquara, São Paulo, Brazil.

^bDepartment of Chemistry, University of Oxford, South Parks Road, Oxford OX1 3QZ, UK.

ABSTRACT: Electrochemical immunosensors offer much in the potential translation of a lab based sensing capability to a useful “real world” platform. We have introduced electrochemical capacitance spectroscopy (ECS), an impedance based approach, as a simple, reagentless, technique capable of reporting on analyte target capture at suitably prepared mixed-component antibody-modified interfaces. Herein we directly integrate receptive aptamers into a redox charging peptide support in establishing a low pM analytical assay for C-Reactive Protein with a sensitivity that significantly exceeds that attainable with an analogous antibody interface.

In recent years, there has been a growing interest in the development of optimized interfaces capable of supporting the detection of clinically relevant analytes¹, especially those translatable to rapid low cost analyses.²⁻⁴ Derived immunosensors^{1,5-7} (which translate a biological biomarker recognition into a measurable signal) have been based on a variety of electrochemical techniques, such as voltammetry⁸, amperometry^{8,9} and electrochemical impedance spectroscopy (EIS)¹⁰⁻¹². EIS is a natively spectroscopic and highly sensitive method¹³ within which interfacial charge transfer resistance R_{ct} is assessed as a reporter of analyte^{14,15}. Recently we introduced electrochemical capacitance spectroscopy (ECS)^{13,16-18}, an EIS-based technique utilising change in interfacial redox capacitance (C_r) as a transducer, omitting the need for a solution phase redox-probe^{14,19-21}. When incorporated into a molecular film capable of selectively binding an analyte, C_r becomes a sensitive function of target concentration. To date such interfaces have been created by covalent immobilization of bio-receptors within a mixed self-assembled monolayer (SAM), one film component being redox active, the second serving as a receptor anchor.

In this work, a surface assembling redox tagged peptide is used to the underlying electrode, anchor an aptamer and subsequently transduce target recognition. Single-stranded DNA or RNA aptamers are a well-known biologically receptive platform^{6,22-29} capable of supporting a diverse array of assays with some notable advantages over antibodies.³⁰⁻³⁴. Herein we demonstrate, not only that the so generated interface exhibits high target selectivity but also that the relatively higher receptor density afforded at peptide-supported aptamer films enables notably higher assay sensitivity.

EXPERIMENTAL SECTION

Chemical Reagents. The synthetic anti-CRP aptamer (5'-CGA AGG GGA TTC GAG GGG TGA TTG CGT GCT CCA TTT GGT GTT TTT TTT TTT T- NH₂ 3') was obtained from the Oxford Aptamer Group. Ultra-pure water was obtained from a Milli-Q 18.2 MΩ×cm system and was used in all solutions. Fmoc-Cys(Trt)-OH, Fmoc-Ala-OH; Fmoc-Glu(OtBu)-OH, Rink Amide resin and 3-ferrocenylpropionic anhydride were purchased from Sigma Aldrich Co. (USA). All solvents and chemicals used were of analytical grade.

Electrochemical Apparatus. An Autolab potentiostat equipped with an FRA32 module (METROHM Instruments) was used for electrochemical measurements. A three-electrode setup was used for the measurements consisting of a 2.0 mm diameter gold working electrode from METROHM, a platinum mesh counter electrode, and a silver/silver chloride (Ag|AgCl, filled with 3.0 M KCl) reference electrode. All potentials reported are relative to a Ag|AgCl reference electrode.

Synthesis of Redox-tagged Peptide. The peptide Fc-Glu-Ala-Ala-Cys was manually produced by solid phase peptide synthesis (SPPS) using Fmoc protocols on an Rink Amide Resin (0.48 mmol g⁻¹). Coupling was performed at a 2-fold molar excess relative to the amino component in the resin, using diisopropylcarbodiimide (Dic)/ 1-hydroxybenzotriazole (HOBt). Fmoc groups were deprotected using 20% N-methylpiperidine/dimethylformamide (DMF) for 20 minutes. The ferrocene redox probe was introduced at the N-terminus by reaction with one molar equivalent 3-ferrocenylpropionic anhydride in 5 mL DCM/DMF (1:1) for 24h. Peptide cleavage from the resin and removal of the side chain protecting groups were performed with 94% TFA, 2.5% 1,2-ethanedithiol, 2.5% H₂O and 1% triisopropylsilane for 2 h. After this, the peptide was precipitated with diethyl ether, separated from soluble non peptide material by centrifugation. The residue was extracted in a 1:1 mixture of solvent A (0.045% (v/v) TFA/H₂O) and solvent B (0.036% (v/v) TFA/ACN) and lyophilized. The crude product was purified by HPLC on a Beckman System Gold using a semi-preparative reverse phase Phenomenex Jupiter C18 column (250 x 10 mm), packed with spherical 5 μm particles and 300 Å pore size. A linear gradient elution was employed from 20 to 50% of solvent B for 90 minutes. The flow rate was 5 mL min⁻¹ at room temperature and the injection volume was 5 mL, UV detection was carried out at 220 nm. The purity of peptide was confirmed (Figure S1) using an analytical Shimadzu system with a reverse phase Phenomenex Jupiter C18 column (150 x 4.6 mm), packed with spherical 5 μm particles and 300 Å pore size, using a linear gradient of 5 to 95 % of solvent B for 30 min, a flow rate of 1.0 mL min⁻¹ and UV detection at 220 nm. The identity of the peptide was analyzed in an ion-trap Mass Spectrometer using a Bruker system in positive mode, confirming the peptide

molecular weight of 635 g/mol (data shown in Supporting Information).

Electrode Prereatment. Gold electrode surfaces were prepared by mechanical polishing with aluminum oxide pads with particle of size of 0.05 μm . Electrodes were electrochemically polished in 0.5 M NaOH between -0.7 V and -1.7 V (500 cycles). The electrodes were immersed in EtOH under stirring for 20 min. A series of wider range scans, from -0.1 to 1.4 V, were then conducted in 0.5 M H_2SO_4 at a scan rate of 0.1 V s^{-1} . The reduction peak of the gold oxide layer formed in the anodic scan was used to calculate the real electroactive area of the electrode.

Sensor Construction. The CRP biosensor was prepared by immersion of the clean Au electrodes in a solution containing 2 mM of redox-tagged peptide in $\text{H}_2\text{O}/\text{ACN}$ (1:1) for 16 hours (25° C). After being thoroughly rinsed with deionized water, the carboxyl groups of the glutamic acid side chain were activated with N-(3-dimethylaminopropyl)-N'-ethylcarbodiimide (EDC)/N-hydroxysuccinimide (NHS), using an aqueous solution containing 0.4 M EDC and 0.1 M NHS for 30 min. The modified electrodes were then incubated in 1 μM anti-CRP aptamer in PBS (solution) (pH 7.4) for 1 h at room temperature, afterwards CV and EIS were performed to confirm the aptamer immobilization. The final step involved incubation in 0.1% BSA solution for 30 minutes to deactivate any remaining active carboxyl groups. A calibration curve was obtained by immersion of the biosensor in PBS (pH 7.4) containing increasing, specific quantities of CRP ranging from 10 pM to 10 nM. The incubation time was 30 min for each concentration and the electrodes were washed with PBS solution before electrochemical analysis. The relative response at various concentrations of CRP was defined as:

$$RR \%_{\text{CRP}} = ((RR_{\text{CRP}} - RR_{\text{Blank}}) \div RR_{\text{Blank}}) \times 100 \quad \text{Eq (1)}$$
where RR_{CRP} is the inverse of redox capacitance ($1/C_r$) at a specific concentration of CRP.

To evaluate the interfacial specificity, the biosensor was incubated in HSA (1 mM) solution for 30 minutes and the redox capacitance measured.

Electrochemical Measurements. All electrochemical measurements were carried out in a cell containing 20 mM TBAClO_4 supporting electrolyte dissolved in acetonitrile and water (1:4 (v/v)). CV was performed at a scan rate of 100 mV s^{-1} between 0.0 V and 0.7 V relative to Ag/AgCl . Electrochemical impedance measurements were carried out in the AC frequency range of 100 kHz to 0.1 Hz with 10 mV amplitude (peak to peak). The DC bias potential was set to the formal potential of the ferrocene redox-tagged peptide (0.36 V, determined by CV). Measurements were verified for com-

pliance with Kramers–Kronig linear systems theory. Electrochemical Capacitance Spectroscopy (ECS) was performed by determining the capacitance, using the relationship $C^*(\omega) = 1/i\omega Z^*(\omega)$, where ω is the angular frequency and i is the complex number $= \sqrt{-1}$.¹⁴

RESULTS AND DISCUSSION

The interface utilised in the present work comprises a simple electrochemically active peptide (Fc-Glu-Ala-Ala-Cys, see chemical structure in Figure S2) sequence obtained through a low cost solid phase synthesis (SPPS³⁵). Synthesis commenced from the C-terminal cysteine, utilised in electrode surface anchoring³⁶. Importantly, upon cleavage of the peptide from the Rink Amide resin the C-terminal carboxy group remained amidated to avoid negative charges close to the surface anchoring site, charges which could impede lateral packing³⁶. Two alanine residues were introduced to promote film crystallinity,³⁶ then a N-terminal glutamic acid integrated. A ferrocene redox-probe was introduced at the N-terminus by reaction with 3-ferrocenylpropionic anhydride while the carboxy side-chain remained unmodified to enable bioconjugation (via, for example EDC/NHS coupling³⁷) after SAM formation. The structure and purity of the peptide was confirmed by mass spectrometry (Figure S1a) and HPLC (purity of >98%, see Figure S1b). The infrared spectrum (Figure S1c) characteristic of amide I band (1654 cm^{-1}) is consistent with a CD supported (not shown) random coil structure.

After peptide self-assembly the interface was investigated by CV and EIS (Figure 1a). The faradaic response has a half-wave (E_{in}) potential of (0.360 ± 0.002) V, a small peak separation (approx. 10 mV) and an expected linear dependence of magnitude on voltage sweep rate (see Figure S5). The molecular surface density was determined by three independent methods (Table S1). The derived mean molecular surface coverage was determined to be $(2.13 \pm 0.70) \times 10^{-10} \text{ mol cm}^{-2}$, in good agreement with prior reports for peptide SAMs^{38–43}. The capacitive redox activity of the interface as evaluated by ECS is shown in Figure 1b. A C_r value of $267.0 \pm 7.1 \mu\text{F cm}^{-2}$ at E_{in} was obtained from the capacitance Nyquist semicircle diameter and is markedly greater than either the capacitance of bare gold ($11.0 \pm 0.8 \mu\text{F cm}^{-2}$) or the SAM at redox out potentials (potentials where no faradaic redox activity can be observed - E_{out} ; $9.0 \pm 0.7 \mu\text{F cm}^{-2}$). In utilising redox output as a transduction of any subsequent binding, it is imperative that signal stability is both understood and adequate. The films utilised herein display a signal output that changes <5% over 6 hours (Figure S6) in the absence of target, a stability comparable to prior reports observed with terminal Fc films.^{44,45}

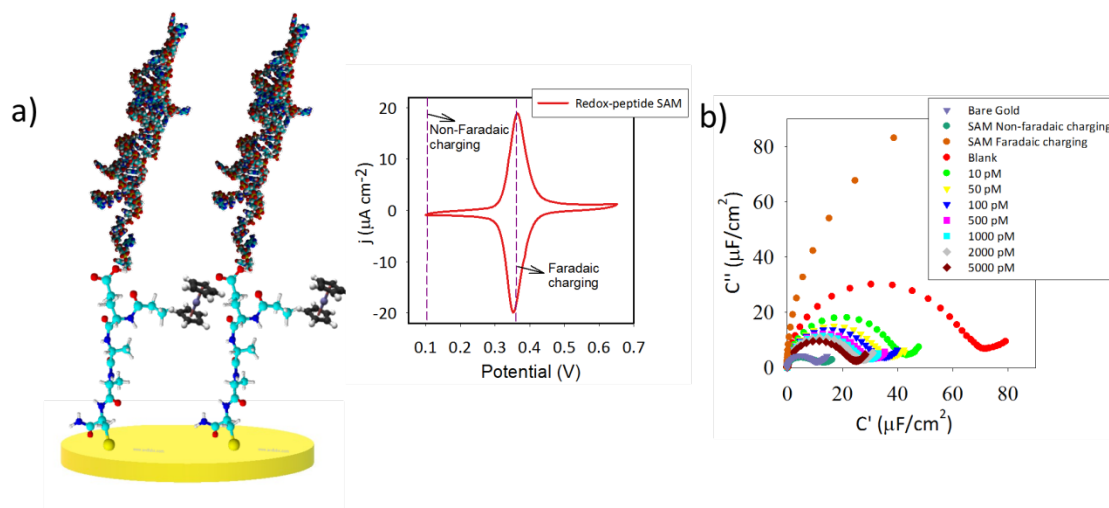


Figure 1. (a) Cyclic voltammogram obtained after redox-tagged peptide SAM formation. Dashed lines represent the non-faradaic charging (0.1 V) and faradaic charging (0.360 V) potentials. CVs were obtained in 20 mM TBAClO₄ in ACN/H₂O 1:4, at a scan rate of 0.1 V s⁻¹. (b) Peptide-supported aptamer biosensor after incubation with various concentrations of CRP. Capacitive Nyquist plots of biosensing interface showing high sensitivity towards CRP.

Upon covalent immobilization of CRP aptamer the redox capacitance (at E_{in}) decreased, indicating successful receptor recruitment (Figure S7)^{19,46,47}. The large ($54 \pm 1\%$) decrease in C_r is indicative of a high aptamer surface density, subsequently quantified by redox tagging⁴⁸ as $7.8 \pm 1.5 \times 10^{11}$ molecules cm⁻², a value considerably higher than possible for an IgG film (8.3×10^9 molecules cm⁻²)⁴⁹. The interface responds sensitively ($87.7 \pm 3.7\%$ per decade) to CRP (Figure 1b) as assessed at the E_{in} potential (0.36 V) across a 10 pM – 5000 pM range. Capacitive analysis performed at E_{out} potentials (0.1 V) is unresponsive to CRP (Figure S8). Furthermore, standard impedimetric analysis (Figure S8a) does not display measurable changes after incubation with CRP, even at very high concentrations⁴⁷.

A comparative analysis of the interfacial response with an analogous anti-CRP mAb receptor is shown in Table S2 where the markedly greater sensitivity afforded by the aptamer is evident. We ascribe this to a combination of its surface density and steric availability^{31,50}.

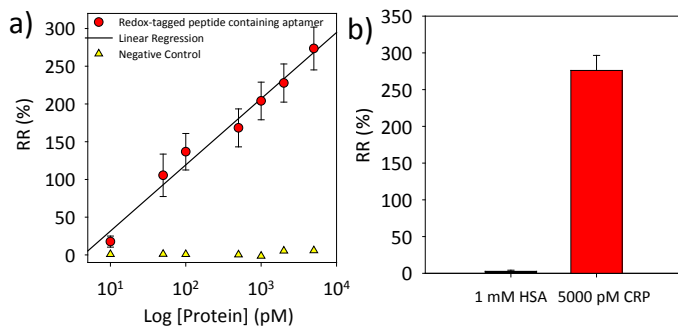


Figure 2. Relative response (RR (%)) of peptide-supported aptamer biosensor as measured by redox capacitance in the presence of proteins. (a) Relative response after incubation with increasing amounts of CRP (red circles) as well as after incubation with BSA (yellow triangles). (b) Comparison of relative response after

incubation with 1 mM HSA or 5 nM CRP. Error bars represent one standard deviation of measurements on three separate electrodes.

Interfacial specificity towards CRP was evaluated by incubation of the aptamer-based biosensor with various concentrations of BSA (bovine serum albumin) and human serum albumin (HSA), which is the most abundant protein in human blood plasma at approximately 35 - 50 g/L⁵¹. As can be seen (Figure 2a). Incubation with high concentrations of HSA (1 mM) does not induce any notable response ($RR\% = 2.6 \pm 1.5\%$) in comparison to that observed with 5 nM CRP $276.0 \pm 20.5\%$ (Figure 2b).

CONCLUSIONS

In summary, this work has introduced a simple and highly sensitive capacitive biosensor for CRP using an aptamer supported peptide interface. The underlying single-component peptide scaffold, incorporating a ferrocene redox transducer as well as a receptor anchor site omits the use of mixed alkanethiol SAMs and can be married with a high-density aptamer coverage to produce a capacitive interface that responds with high sensitivity to target. The redox supported aptamer films have a sensory response that compares favourably with related aptamer work, including that with redox tagged aptamers,⁵² (Table S3) with the advantage herein that transduction is stable, reagentless and requires no prior modification of the receptive entity.

ASSOCIATED CONTENT

Supporting Information

Further information about peptide characterization, surface density coverage and biosensor construction can be found in the SI.

AUTHOR INFORMATION

Corresponding Author

*jason.davis@chem.ox.ac.uk, tel: +44 1865 275914, Department of Chemistry, University of Oxford, South Parks Road, Oxford OX1 3QZ, United Kingdom

#prbueno@iq.unesp.br, tel: +55 16 3301 9642, fax: +55 16 3322 2308, Instituto de Química, Universidade Estadual Paulista, CP 355, 14800-900 Araraquara, São Paulo, Brazil

Notes

The authors declare no competing financial interest.

ACKNOWLEDGMENT

Julia P. Piccoli acknowledges CAPES for her scholarship.

REFERENCES

- (1) Bohunicky, B.; Mousa, S. A. *Nanotechnol Sci Appl* **2010**, *4*, 1-10.
- (2) Campuzano, S.; Yáñez-Sedeño, P.; Pingarrón, J. M. *Diagnostics (Basel)* **2016**, *7*.
- (3) Pultar, J.; Sauer, U.; Domnanich, P.; Preininger, C. *Biosens Bioelectron* **2009**, *24*, 1456-1461.
- (4) Wulfschuh, J. D.; Liotta, L. A.; Petricoin, E. F. *Nat Rev Cancer* **2003**, *3*, 267-275.
- (5) *Sensors and Actuators B: Chemical* **2017**, *244*, 742 - 749.
- (6) Bini, A.; Centi, S.; Tombelli, S.; Minunni, M.; Mascini, M. *Anal Bioanal Chem* **2008**, *390*, 1077-1086.
- (7) Daniels, J. S.; Pourmand, N. *Electroanalysis* **2007**, *19*, 1239-1257.
- (8) Turner, A.; Karube, I.; Wilson, G. S. **1987**.
- (9) Karyakin, A. A.; Gitelmacher, O. V.; Karyakina, E. E. *Analytical Letters* **1994**, *27*, 2861-2869 % @ 0003-2719.
- (10) Chang, B.-Y.; Park, S.-M. *Annual Review of Analytical Chemistry* **2010**, *3*, 207-229 % @ 1936-1327.
- (11) Lisdat, F.; Schäfer, D. *Analytical and bioanalytical chemistry* **2008**, *391*, 1555 % @ 1618-2642.
- (12) Bogomolova, A.; Komarova, E.; Reber, K.; Gerasimov, T.; Yavuz, O.; Bhatt, S.; Aldissi, M. *Analytical chemistry* **2009**, *81*, 3944-3949 % @ 0003-2700.
- (13) Bueno, P. R.; Fabregat-Santiago, F.; Davis, J. J. *Anal Chem* **2013**, *85*, 411-417.
- (14) Bueno, P. R.; Mizzon, G.; Davis, J. J. *J Phys Chem B* **2012**, *116*, 8822-8829.
- (15) Barton, A. C.; Davis, F.; Higson, S. a. P. J. *Analytical chemistry* **2008**, *80*, 6198-6205 % @ 0003-2700.
- (16) Bedatty Fernandes, F. C.; Patil, A. V.; Bueno, P. R.; Davis, J. J. *Anal Chem* **2015**, *87*, 12137-12144.
- (17) Berggren, C.; Johansson, G. *Analytical Chemistry* **1997**, *69*, 3651-3657 % @ 0003-2700.
- (18) Bueno, P. R.; Davis, J. J. *Anal Chem* **2014**, *86*, 1337-1341.
- (19) Fernandes, F. C.; Góes, M. S.; Davis, J. J.; Bueno, P. R. *Biosens Bioelectron* **2013**, *50*, 437-440.
- (20) Góes, M. S.; Rahman, H.; Ryall, J.; Davis, J. J.; Bueno, P. R. *Langmuir* **2012**, *28*, 9689-9699.
- (21) Lehr, J.; Hobnouse, G. C.; Fernandes, F. C.; Bueno, P. R.; Davis, J. J. *Anal Chem* **2014**, *86*, 2559-2564.
- (22) Citartan, M.; Gopinath, S. C.; Tominaga, J.; Tan, S. C.; Tang, T. H. *Biosens Bioelectron* **2012**, *34*, 1-11.
- (23) Daniel, J.; Fetter, L.; Jett, S.; Rowland, T. J.; Bonham, A. J. *Methods Mol Biol* **2017**, *1600*, 9-23.
- (24) Fetter, L.; Richards, J.; Daniel, J.; Roon, L.; Rowland, T. J.; Bonham, A. J. *Chem Commun (Camb)* **2015**, *51*, 15137-15140.
- (25) Förster, C.; Zydek, M.; Rothkegel, M.; Wu, Z.; Gallin, C.; Geßner, R.; Lisdat, F.; Fürste, J. P. *Biochem Biophys Res Commun* **2012**, *419*, 60-65.
- (26) Seo, H. B.; Gu, M. B. *J Biol Eng* **2017**, *11*, 11.
- (27) Vance, S. A.; Sandros, M. G. *Sci Rep* **2014**, *4*, 5129.
- (28) Wang, J.; Guo, J.; Zhang, J.; Zhang, W.; Zhang, Y. *Biosens Bioelectron* **2017**, *95*, 100-105.
- (29) Zhang, Z.; Yang, W.; Wang, J.; Yang, C.; Yang, F.; Yang, X. *Talanta* **2009**, *78*, 1240-1245.
- (30) Wu, B.; Jiang, R.; Wang, Q.; Huang, J.; Yang, X.; Wang, K.; Li, W.; Chen, N.; Li, Q. *Chem Commun (Camb)* **2016**, *52*, 3568-3571.
- (31) Jayasena, S. D. *Clinical chemistry* **1999**, *45*, 1628-1650 % @ 0009-9147.
- (32) Poolsup, S.; Kim, C.-Y. *Current Opinion in Biotechnology* **2017**, *48*, 180-186 % @ 0958-1669.
- (33) Urmann, K.; Modrejewski, J.; Scheper, T.; Walter, J.-G. *BioNanoMaterials* **2017**, *18*.
- (34) Bernardes, G. J. L.; Steiner, M.; Hartmann, I.; Neri, D.; Cusi, G. *Nat. Protocols* **2013**, *8*, 2079-2089.
- (35) Merrifield, R. B. *J. Am. Chem. Soc.* **1963**, *85*, 2149-2154.
- (36) Nowinski, A. K.; Sun, F.; White, A. D.; Keefe, A. J.; Jiang, S. *J Am Chem Soc* **2012**, *134*, 6000-6005.
- (37) Girardot, J. M.; Girardot, M. N. *J Heart Valve Dis* **1996**, *5*, 518-525.
- (38) Morita, T.; Kimura, S. *J Am Chem Soc* **2003**, *125*, 8732-8733.
- (39) *Biosensors and Bioelectronics* **2016**, *84*, 82 - 88.
- (40) Anita J. Zaitouna, A. J. M.; Rebecca Y. Lai. *Analytica Chimica Acta* **2015**, *886*, 157 - 164.
- (41) Gatto, E.; Porchetta, A.; Scarselli, M.; De Crescenzi, M.; Formaggio, F.; Toniolo, C.; Venanzi, M. *Langmuir* **2012**, *28*, 2817-2826 % @ 0743-7463.
- (42) Gatto, E.; Venanzi, M. *Polymer journal* **2013**, *45*, 468-480.
- (43) Longo, E.; Wright, K.; Caruso, M.; Gatto, E.; Palleschi, A.; Scarselli, M.; De Crescenzi, M.; Crisma, M.; Formaggio, F.; Toniolo, C.; Venanzi, M. *Nanoscale* **2015**, *7*, 15495-15506.
- (44) Kang, D.; Ricci, F.; White, R. J.; Plaxco, K. W. *Analytical chemistry* **2016**, *88*, 10452-10458 % @ 10003-12700.
- (45) Beulen, M. W. J.; Kastenbergh, M. I.; van Veggel, F. C. J. M.; Reinhoudt, D. N. *Langmuir* **1998**, *14*, 7463-7467 % @ 0743-7463.
- (46) Bueno, P. R.; Fabregat-Santiago, F.; Davis, J. J. *Analytical chemistry* **2012**, *85*, 411-417.
- (47) Fernandes, F. C.; Santos, A.; Martins, D. C.; Góes, M. S.; Bueno, P. R. *Biosens Bioelectron* **2014**, *57*, 96-102.
- (48) Yu, H.-Z.; Luo, C.-Y.; Sankar, C. G.; Sen, D. *Analytical chemistry* **2003**, *75*, 3902-3907 % @ 0003-2700.
- (49) Jmol. The CRP antibody footprint was determined as 114 x 105 nm with Jmol.
- (50) Balamurugan, S.; Obubuafo, A.; Soper, S. A.; Spivak, D. A. *Analytical and bioanalytical chemistry* **2008**, *390*, 1009-1021 % @ 1618-2642.
- (51) McPherson, R. A.; Pincus, M. R. *Henry's Clinical Diagnosis and Management by Laboratory Methods E-Book*; Elsevier Health Sciences, 2017.
- (52) Lai, R. Y.; Plaxco, K. W.; Heeger, A. J. *Analytical chemistry* **2007**, *79*, 229-233 % @ 0003-2700.

Insert Table of Contents artwork here

